Journal of Constructional Steel Research 64 (2008) 1275–1282

Contents lists available at ScienceDirect

Journal of Constructional Steel Research

journal homepage: www.elsevier.com/locate/jcsr

Structural design of stainless steel concrete filled columns

Dennis Lam [a,*], Leroy Gardner [b]

[a] *School of Civil Engineering, University of Leeds, Leeds, LS2 9JT, UK*

[b] *Department of Civil and Environmental Engineering, Imperial College, London, SW7 2AZ, UK*

ARTICLE INFO

Article history:
Received 12 November 2007
Accepted 30 April 2008

Keywords:
CHS
Composite column
Concrete filled
Confinement
Deformation-based
Local buckling
SHS
Stainless steel
Tubular construction

ABSTRACT

This paper presents the behaviour and design of axially loaded concrete filled stainless steel circular and square hollow sections. The experimental investigation was conducted using different concrete cube strengths varied from 30 to 100 MPa. The column strengths and load-axial shortening curves were evaluated. The study is limited to cross-section capacity and has not been validated at member level. Comparisons of the tests results together with other available results from the literature have been made with existing design methods for composite carbon steel sections — Eurocode 4 and ACI. It was found that existing design guidance for carbon steel may generally be safely applied to concrete filled stainless steel tubes, though it tends to be over-conservative. A continuous strength method is proposed and it is found to provide the most accurate and consistent prediction of the axial capacity of the composite concrete filled stainless steel hollow sections due largely to the more precise assessment of the contribution of the stainless steel tube to the composite resistance.

1. Introduction

Concrete filled tubes (CFT) are gaining increasing usage in modern construction practice throughout the world, particularly in Australia and the Far East. This increase in use is largely due to the structural and economical advantages offered by concrete filled tubes over open and empty sections, as well as their aesthetic appeal. From a structural viewpoint, hollow sections exhibit high torsional and compressive resistance about all axes when compared with the open sections. Additionally, the exposed surface area of a closed section is approximately two-thirds that of a similar sized open section, thus demanding lower painting and fireproofing costs [1].

Composite columns comprise a combination of concrete and steel and utilise the most favourable properties of the constituent materials. Use of composite columns can result in significant savings in column size, which ultimately can lead to considerable economic savings. This reduction in column size provides is particularly beneficial where floor space is at a premium, such as in car parks and office blocks. The use of stainless steel columns filled with concrete is relatively new and innovative, and not only provides the advantages outlined above but also brings the durability associated with stainless steel.

The term 'composite column' refers to a compression member in which the steel and concrete elements act compositely. The role of the concrete core in a composite column is not only to resist compressive forces but also to reduce the potential for buckling of the steel member. The steel tube reinforces the concrete to resist any tensile forces, bending moments and shear forces, and offers confinement to the concrete. Composite columns can buckle in local or overall modes, but this investigation is focused on the cross-section resistance of short composite columns, where only local buckling effects were exhibited.

Unlike carbon steel, stainless steel possesses natural corrosion resistance; significantly, this means that, appropriately specified, the surface can be exposed without the need for any protective coatings. The principal disincentive for the utilisation of stainless steel for structural elements is the high initial material cost, but, considered on a whole-life basis, cost comparisons with other metallic materials become more favourable [2]. Concrete infilling on stainless steel tubes maintains the durable and aesthetic exposed surface, but will lead to reduced column sizes and material thickness, both of which have clear economic incentives.

The main objective of this research program is to investigate the compressive behaviour of composite stainless steel concrete filled columns with concrete infill strengths of 30, 60 and 100 MPa. The compressive resistances are compared with those attained from unfilled stainless steel hollow sections. Further comparisons are made with existing design rules based on Eurocode 4 [3] and ACI-318 [4]. New design expressions based on the Continuous Strength Method to determine the strength and contribution of the stainless steel are also proposed.

* Corresponding author. Tel.: +44 113 343 2295; fax: +44 113 343 2265.
E-mail address: d.lam@leeds.ac.uk (D. Lam).

0143-974X/$ – see front matter © 2008 Elsevier Ltd. All rights reserved.
doi:10.1016/j.jcsr.2008.04.012

2. Past research

Composite columns have been used for over 100 years, initially to provide fire protection to steel structures. Later, the strength properties were also taken into account when designing concrete encased columns, but it was not until the 1960s that research into concrete filled steel tubes began. A state of the art review reported by Shanmugam and Lakshmi [5] on steel–concrete composite columns has highlighted the significant research in this area. The majority of research to date has been focused on the capacity, fire resistance, and seismic resistance of carbon steel composite columns, with numerous models proposed for the prediction of structural behaviour.

Experimental studies on the behaviour of short composite columns with circular hollow sections (CHS) concentrically loaded in compression have been carried out by Schneider [6], Lam and Giakoumelis [7], and O'Shea and Bridge [8,9] to investigate the effect of steel tube shape and wall thickness on ultimate capacity. The results have suggested that CHS offer substantial post-yield stiffness and ductility that are not available in square or rectangular hollow sections. Lam and Giakoumelis [7] also assessed concrete filled tubes under different loading conditions — on the concrete and steel simultaneously, the concrete alone and the concrete and steel with a greased column. Results indicated that when the concrete and steel were loaded simultaneously, the tube provided little confinement in comparison to the concrete only loaded specimens; similar findings were also reported by Sakino et al. [10].

Concrete compaction was identified as playing a key role in the performance of concrete filled tubes by Han and Yang [11] and Han and Yao [12]. Tests on concrete filled carbon steel tubes were carried out to determine the influence of compaction methods on column capacity. The tests confirmed that better compaction resulted in higher section capacities and highlighted the importance of concrete compaction on the performance of composite concrete filled CHS. It was also noted that self-consolidating concrete (SCC) is being increasingly used in concrete filled tubular columns since this can avoid the need for vibro-compaction while still achieving good consolidation.

An investigation into the use of high strength material in composite columns was reported by Uy [13]. It was stated that the use of high strength materials may provide many benefits in multi-storey construction including reduced column sizes and a subsequent increase in lettable floor area. Gibbons and Scott [14] found that utilising high strength concrete results in increased stiffness and hence reduced section sizes for columns designed for slenderness effects and lateral loading. Research into thin-walled carbon steel tubes with high strength concrete infill has been carried out by Rangan and Joyce [15], O'Shea and Bridge [16], and Kilpatrick and Rangan [17]. Strength enhancement and improved ductility provided by the confined concrete was confirmed, but it was reported that the concrete infill had little effect on the local buckling strength of the steel tube.

Studies of carbon steel rectangular hollow section (RHS) composite columns have been performed by Uy [18–20], Han and Yao [21], Mursi and Uy [22], Lam and Williams [23], and Han [24]. Experimental results on the strength, local and post-local buckling behaviour were reported. The results have indicated that the width-to-thickness ratio of the steel elements and the constraining factor (the ratio of the component resistances of the composite column) both have a significant influence on the compressive load carrying capacity and ductility of the concrete filled columns.

Recent years have seen extensive studies into the structural performance of unfilled stainless steel hollow sections, these being the most widely used structural stainless steel cross-section type [25]. Notable early studies were reported by Rasmussen and Hancock [26,27], and Talja and Salmi [28], who investigated the compressive and flexural response of stainless steel hollow sections, whilst a series of more recent investigations have now been performed [29–33]. These studies have contributed to a growing pool of structural performance data on stainless steel elements, and have highlighted some shortcomings in existing design guidance. In particular, the rounded stress–strain curve and strong strain hardening characteristics exhibited by stainless steel have been essentially disregarded in current structural design codes, in favour of a simplified treatment involving use of the 0.2% proof stress and a bi-linear (elastic, perfectly plastic) material model — this leads to significant conservatisms, most notably for stocky elements. A new, more rational and efficient approach to structural stainless steel design, which takes due account of the particular stress–strain characteristics of stainless steel, has been developed [34–36], and its applicability to concrete filled stainless steel tubes will be assessed in this paper. The structural behaviour of high strength stainless steel tubular members has been studied by Young and Lui [37], Ellobody and Young [38], and Gardner, Talja and Baddoo [39]; these studies have led to an expansion of the scope of Eurocode 3: Part 1.4 [40] to now cover cold-worked stainless steel grades.

Previous research into the structural behaviour and design of concrete filled stainless steel tubes has been rather limited, with the only reported studies to date by Young and Ellobody [41], and Ellobody and Young [42]. The results from these studies are analysed in this paper.

3. Experimental study

3.1. Introduction

An experimental study was performed to assess the compressive response of stainless steel concrete filled tubular columns. Two cross-section types were investigated — square hollow sections (SHS) and circular hollow sections (CHS). Tests were performed on four different section sizes — SHS 100 × 100 × 5, SHS 100 × 100 × 2, CHS 114 × 6 and CHS 104 × 2. For each section size, four stub column tests were carried out — one on the empty stainless steel tube and three concrete filled specimens with nominal concrete strengths of 30, 60 and 100 MPa. Tests were also conducted on the constituent materials — tensile tests on coupons extracted from the stainless steel tubes and cube and cylinder tests on the concrete.

3.2. Concrete material properties

Three nominal concrete strengths – C30, C60, and C100 – were studied. The concrete was produced using commercially available materials with normal mixing and curing techniques; the three mix designs are shown in Table 1. The strength development of the concrete was monitored over a duration of 28 days by conducting periodic cube and cylinder tests — the results of the cube tests are illustrated in Fig. 1. Additionally, at the time of each series of stub column tests, two further standard cube tests and two standard cylinder tests were performed. For the SHS tests, the mean measured cube strengths for the C30, C60, and C100 concrete were 37, 66 and 92 MPa, whilst the corresponding cylinder strengths were 30, 53 and 74 MPa. For the CHS tests, the equivalent mean measured cube strengths were 42, 67 and 97 MPa, whilst the corresponding cylinder strengths were 31, 49 and 65 MPa. The cylinder strengths are employed in the design model comparisons presented in Section 4 of this paper.

Table 1
Mix design for C30, C60, and C100 concrete

Nominal concrete strength	Water/cement ratio	Mix proportions (to weight of cement)					
		Cement	Coarse	Fine	Water	Silica	Plasticiser
C30	0.65	1.0	3.5	3.0	0.65	–	–
C60	0.42	1.0	3.25	2.0	0.42	–	–
C100	0.28	1.0	2.5	1.5	0.28	0.1	2%

Table 2
Measured stainless steel material properties

Specimen	E (N/mm^2)	$\sigma_{0.2}$ (N/mm^2)	$\sigma_{1.0}$ (N/mm^2)	σ_u (N/mm^2)	n	$n'_{0.2,1.0}$
SHS 100 × 100 × 2 – TC1	202 500	385	456	481	12.4	4.0
SHS 100 × 100 × 5 – TC1	180 000	458	610	632	3.7	3.6
CHS 104 × 2 – TC1	191 200	412	469	628	4.5	2.7
CHS 104 × 2 – TC2	192 600	412	485	634	4.0	3.2
CHS 114 × 6 – TC1	180 100	257	296	544	10.8	2.0
CHS 114 × 6 – TC2	187 100	275	326	534	6.0	2.3

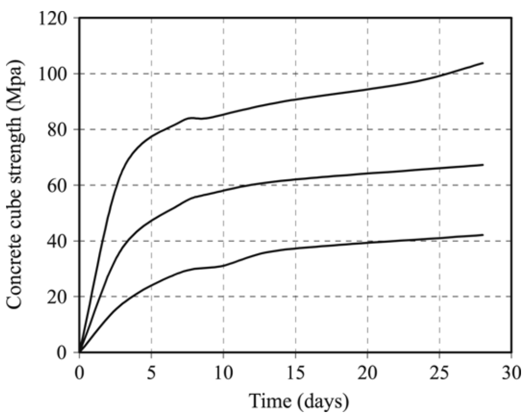

Fig. 1. Cube strength development of C30, C60, and C100 concrete.

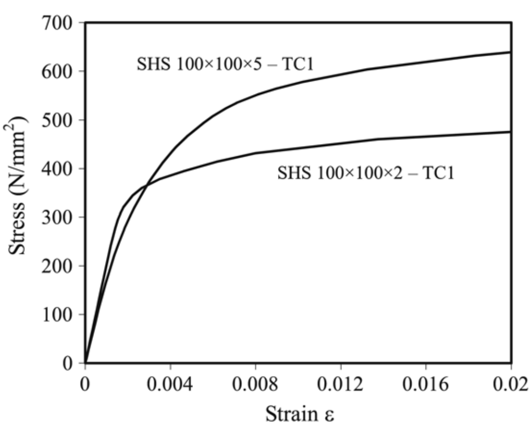

Fig. 2. Stress–strain curves for SHS material.

3.3. Stainless steel material properties

Tensile coupons were machined from the stainless steel sections and tested to determine the basic material stress–strain characteristics. A total of six tensile coupon tests were performed — one for each of the SHS sizes, and two for each of the CHS sizes. For the coupons cut from the CHS, some flattening of the ends of the samples occurred during gripping, but this was remote from the necked region and believed not to influence the resulting stress–strain characteristics. The tests were carried out in accordance with EN 10002-1 [43]. The measured tensile stress–strain curves are shown in Fig. 2 for the SHS coupons and Fig. 3 for the CHS coupons. The notation 'TC1' and 'TC2' refers to tensile coupon 1 and 2. The key material parameters have been summarised in Table 2, where E is the initial tangent (Young's) modulus, $\sigma_{0.2}$ and $\sigma_{1.0}$ are the 0.2% and 1.0% proof strengths respectively, σ_u is the ultimate tensile strength, and n and $n'_{0.2,1.0}$ are strain hardening exponents for the compound Ramberg–Osgood material model described in [34]. This adopted compound Ramberg–Osgood model was developed on the basis of a two-stage version of the original Ramberg–Osgood expression [44,45], proposed in [46,47].

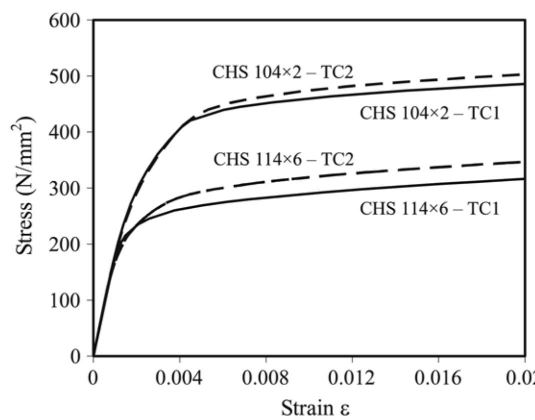

Fig. 3. Stress–strain curves for CHS material.

3.4. Stub column tests

A total of 16 stub column tests were performed — one empty tube and three concrete filled tubes (with 30, 60, and 100 MPa concrete) for each of the four section sizes. The measured dimensions of the SHS and CHS stub column specimens are listed in Tables 3 and 4, respectively. Effective areas A_{eff}, calculated according to Eurocode 3: Part 1.5 [48], have been tabulated for the slender SHS, whilst all CHS are fully effective. All stub columns were 300 mm in length — this length was chosen to ensure that the specimens were sufficiently short not to fail by overall flexural buckling, yet still suitably long to contain representative distributions of residual stresses and geometric imperfections [49]. Clamps were employed at each end of the specimens to reduce end effects and to encourage failure in the region of the strain gauges. The clamps themselves were located fractionally away from the ends of the specimens to ensure that no load was transferred into the stainless steel tubes by the clamps. In order to fill any voids and achieve uniform compressive loading on the stub columns, a thin layer of plaster was applied to the two ends of the specimens and

Table 3
Geometric properties of SHS stub column test specimens

Section	Depth D (mm)	Breadth B (mm)	Thickness t (mm)	A_s (mm^2)	A_{eff} (mm^2)	A_c (mm^2)
SHS 100 × 100 × 2 (Empty)	100.7	100.8	2.00	780	494	–
SHS 100 × 100 × 2 – C30	100.2	101.6	2.20	856	587	9308
SHS 100 × 100 × 2 – C60	101.3	99.3	2.00	776	494	9269
SHS 100 × 100 × 2 – C100	99.8	101.0	2.20	852	587	9211
SHS 100 × 100 × 5 (Empty)	100.6	100.1	4.80	1775	1775	–
SHS 100 × 100 × 5 – C30	99.9	100.6	5.00	1841	1841	8123
SHS 100 × 100 × 5 – C60	100.5	99.9	4.90	1806	1806	8151
SHS 100 × 100 × 5 – C100	100.6	99.9	4.90	1807	1807	8160

Table 4
Geometric properties of CHS stub column test specimens

Section	Outer diameter D (mm)	Thickness t (mm)	A_s (mm^2)	A_c (mm^2)
CHS 104 × 2 (Empty)	104.0	2.00	641	–
CHS 104 × 2 – C30	104.0	2.00	641	7854
CHS 104 × 2 – C60	104.0	2.00	641	7854
CHS 104 × 2 – C100	104.0	2.00	641	7854
CHS 114 × 6 (Empty)	114.3	6.02	2048	–
CHS 114 × 6 – C30	114.3	6.02	2048	8213
CHS 114 × 6 – C60	114.3	6.02	2048	8213
CHS 114 × 6 – C100	114.3	6.02	2048	8213

(a) Test set-up for SHS stub columns. (b) Test set-up for CHS stub columns.

Fig. 4. Test arrangement for stub column tests.

allowed to harden under a pre-load of 20 kN. A minimum amount of plaster was employed in order to limit its influence on the initial stages of loading. Two longitudinally aligned strain gauges were affixed to all stub columns at mid-height, whilst a third radially orientated strain gauge was employed on the CHS. Two linear variable displacement transducers were located either side of the stub columns to measure the end shortening. The experimental arrangement is shown in Fig. 4.

The tests were conducted using a 3000 kN capacity Toni Pack 3000 testing machine and in accordance with the general recommendations of the Structural Stability Research Council [49]. Each specimen was loaded manually at a rate of approximately 3 kN/s and data were logged at 10 kN intervals.

The load-end shortening curves from the SHS stub column tests are shown in Figs. 5 and 6, whilst those from the CHS tests are shown in Figs. 7 and 8. Typical failure modes of the composite stub columns, featuring outward local buckling of the stainless steel sections, are shown in Fig. 9. The results show the clear advantage of composite stainless steel columns over their bare (unfilled) stainless steel counterparts. Overall, it may be observed from Figs. 5–8 that the stockier stainless steel tubes and lower concrete strengths have more ductile behaviour, though enhancements in load carrying capacity beyond that of the bare stainless steel sections due to concrete filling are more significant for slender sections and higher concrete strengths. The ultimate loads from the stub columns tests N_{Test} are presented in Tables 5 and 6. Note that for the stocky CHS, the ultimate loads were, in some cases, reached following large plastic deformations; for comparison, the ultimate loads achieved prior to or at a maximum strain limit of 5% $N_{Test(5\%)}$ have also been tabulated.

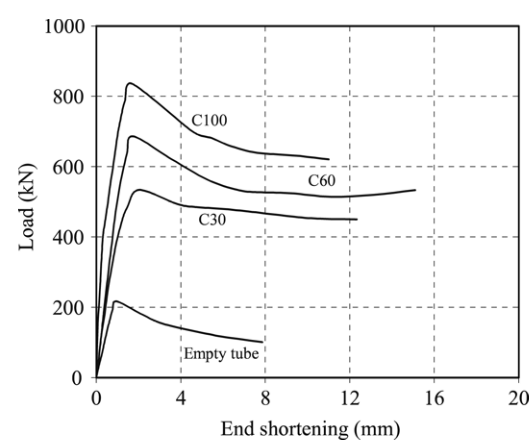

Fig. 5. Load-end shortening response for SHS 100 × 100 × 2 composite stub columns.

Table 5
Comparison of SHS and RHS test results with design models

Section	f_y ($\sigma_{0.2}$) (N/mm^2)	f_c (MPa)	N_{Test} (kN)	$\frac{N_{Test}}{N_{EC4}}$ Eq. (1)	$\frac{N_{Test}}{N_{ACI}}$ Eq. (6)	$\frac{N_{Test}}{N_{CSM}}$ Eq. (10)	$\frac{N_{Test}}{N_{CSM,Mod}}$ Eq. (12)
SHS 100 × 100 × 2 (Empty)	385	–	217	1.14	0.95	0.93	0.93
SHS 100 × 100 × 2 – C30	385	30	534	1.06	1.06	0.96	0.99
SHS 100 × 100 × 2 – C60	385	53	687	1.01	1.07	0.96	1.02
SHS 100 × 100 × 2 – C100	385	74	836	0.92	0.99	0.87	0.95
SHS 100 × 100 × 5 (Empty)	458	–	1136	1.40	1.40	1.09	1.09
SHS 100 × 100 × 5 – C30	458	30	1410	1.30	1.35	1.05	1.09
SHS 100 × 100 × 5 – C60	458	53	1488	1.19	1.25	0.99	1.05
SHS 100 × 100 × 5 – C100	458	74	1559	1.09	1.16	0.93	1.01
SHS 150 × 150 × 6 (Empty)[a]	497	–	1927	1.22	1.17	0.99	0.99
SHS 150 × 150 × 6 – C40[a]	497	46.6	2768	1.12	1.15	0.97	1.03
SHS 150 × 150 × 6 – C60[a]	497	61.9	2972	1.08	1.12	0.95	1.02
SHS 150 × 150 × 6 – C80[a]	497	83.5	3020	0.95	1.01	0.85	0.94
SHS 150 × 150 × 3 (Empty)[a]	448	–	409	0.99	0.82	0.83	0.83
SHS 150 × 150 × 3 – C40[a]	448	46.6	1382	0.99	1.04	0.94	0.99
SHS 150 × 150 × 3 – C60[a]	448	61.9	1620	0.95	1.01	0.91	0.97
SHS 150 × 150 × 3 – C80[a]	448	83.5	1851	0.86	0.93	0.83	0.91
RHS 200 × 110 × 4 (Empty)[a]	503	–	957	1.09	0.99	1.13	1.13
RHS 200 × 110 × 4 – C40[a]	503	46.6	1627	0.91	0.93	0.93	0.98
RHS 200 × 110 × 4 – C80[a]	503	83.5	2180	0.88	0.94	0.89	0.98
RHS 160 × 80 × 4 (Empty)[a]	536	–	537	1.11	0.99	1.20	1.20
RHS 160 × 80 × 3 – C40[a]	536	46.6	882	0.85	0.87	0.88	0.92
RHS 160 × 80 × 3 – C60[a]	536	61.9	1015	0.84	0.88	0.86	0.93
RHS 160 × 80 × 3 – C80[a]	536	83.5	1280	0.88	0.94	0.90	0.99
RHS 140 × 80 × 4 (Empty)[a]	486	–	558	1.14	1.04	1.13	1.13
RHS 140 × 80 × 3 – C40[a]	486	46.6	1049	1.09	1.12	1.09	1.15
RHS 140 × 80 × 3 – C60[a]	486	61.9	1097	0.99	1.03	0.98	1.06
RHS 140 × 80 × 3 – C80[a]	486	83.5	1259	0.95	1.01	0.95	1.05
Mean (Unfilled tubes)				1.16	1.05	1.04	1.04
St. Dev. (Unfilled tubes)				0.13	0.18	0.13	0.13
Mean (Filled tubes)				**1.00**	**1.04**	**0.93**	**1.00**
St. Dev. (Filled tubes)				**0.12**	**0.12**	**0.07**	**0.06**
Mean (All tubes)				1.04	1.04	0.96	1.01
St. Dev. (All tubes)				0.14	0.14	0.10	0.08

[a] Test results reported in [41].

Table 6
Comparison of CHS test results with design models

Section	f_y ($\sigma_{0.2}$) (N/mm^2)	f_c (MPa)	N_{Test} (kN)	$N_{Test(5\%)}$ (kN)	$\frac{N_{Test(5\%)}}{N_{EC4}}$ Eq. (1)	$\frac{N_{Test(5\%)}}{N_{EC4,CHS}}$ Eq. (3)	$\frac{N_{Test(5\%)}}{N_{ACI}}$ Eq. (6)	$\frac{N_{Test(5\%)}}{N_{CSM}}$ Eq. (10)	$\frac{N_{Test(5\%)}}{N_{CSM,CHS}}$ Eq. (11)
CHS 104 × 2 (Empty)	412	–	328	328	1.24	1.24	1.24	1.05	1.05
CHS 104 × 2 – C30	412	31	699	699	1.38	1.02	1.48	1.26	0.97
CHS 104 × 2 – C60	412	49	901	901	1.39	1.10	1.52	1.29	1.05
CHS 104 × 2 – C100	412	65	1133	1133	1.46	1.21	1.62	1.38	1.16
CHS 114 × 6 (Empty)	266	–	1062	778	1.43	1.43	1.43	1.06	1.06
CHS 114 × 6 – C30	266	31	1593	1254	1.57	1.11	1.65	1.27	0.98
CHS 114 × 6 – C60	266	49	1648	1340	1.41	1.05	1.51	1.18	0.94
CHS 114 × 6 – C100	266	65	1674	1674	1.55	1.19	1.68	1.32	1.08
Mean (Unfilled tubes)					1.34	1.34	1.34	1.06	1.06
St. Dev. (Unfilled tubes)					0.13	0.13	0.13	0.01	0.01
Mean (Filled tubes)					**1.46**	**1.11**	**1.58**	**1.28**	**1.03**
St. Dev. (Filled tubes)					**0.08**	**0.07**	**0.08**	**0.07**	**0.08**
Mean (All tubes)					1.43	1.17	1.52	1.23	1.04
St. Dev. (All tubes)					0.10	0.13	0.14	0.12	0.07

4. Development of design rules

4.1. Introduction

In this section, the test results presented herein and those reported by Young and Ellobody [41] and Ellobody and Young [42] are compared with current international design rules for composite carbon steel columns, and with a new design approach recently devised for stainless steel structural components. For the comparisons made in this section, all partial safety factors have been set equal to unity (and therefore excluded from the design expressions presented), and the material properties have been taken as their measured values (thus no distinction has been made between characteristic and design strengths in the design expressions presented). This enables a direct comparison between the design models and the test results.

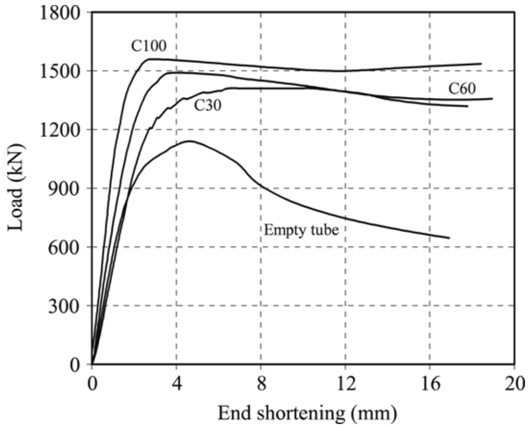

Fig. 6. Load-end shortening response for SHS 100 × 100 × 5 composite stub columns.

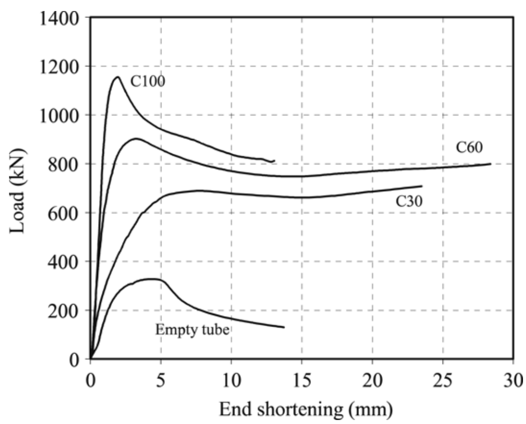

Fig. 7. Load-end shortening response for CHS 104 × 2 composite stub columns.

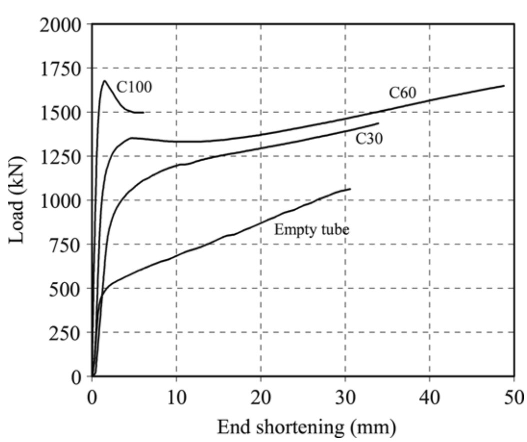

Fig. 8. Load-end shortening response for CHS 114 × 6 composite stub columns.

4.2. Eurocode

The compressive design resistance of concrete filled carbon steel tubes according to Eurocode 4 is given by Eq. (1). Eq. (1) may be applied to SHS and CHS, but a more sophisticated expression, allowing for the effects of concrete confinement, is also provided for CHS only (Eq. (3)). For concrete filled SHS, the compressive design resistance N_{EC4} is defined by a simple summation of the steel and concrete contributions.

$$N_{EC4} = A_c f_c + A_s f_y \tag{1}$$

where A_c is the cross-sectional area of the concrete, f_c is the compressive concrete cylinder strength, A_s is the cross-sectional area of the steel tube and f_y is the yield strength of the steel. For the comparisons with stainless steel test data presented herein, the yield strength has been taken equal to the material 0.2% proof strength $\sigma_{0.2}$. For RHS, the gross cross-sectional area of the steel tube is used, provided the maximum h/t ratio (where h is the width of the section measured to the outer faces and t is the section thickness) is less than or equal to 52ε, where $\varepsilon = (235/f_y)^{0.5}$. This limit is more relaxed than the Class 3 slenderness limit for unfilled tubes, which is defined in Eurocode 3 as 42ε. This is not, however, a direct comparison since the definition of width-to-thickness ratio in Eurocode 3 is based on the flat width of plate c between corner radii — i.e. $c = h - 2t - 2r$, where r is the internal corner radius of the section (typically approximately equal to the material thickness for cold-rolled stainless steel SHS and RHS). It may also be assumed that similar limits can apply to stainless steel [50] SHS and RHS with the modified expression for ε (termed herein as ε_{ss} to distinguish it from the basic carbon steel definition) to account for differences in material stiffness, given by Eq. (2). For CHS, the slenderness limit beyond which local buckling needs to be explicitly accounted for (through the calculation of an effective

(a) SHS.

(b) CHS.

Fig. 9. Typical failure modes of the composite stub columns.

area A_{eff}) is $90\varepsilon^2$, regardless of whether the tube is filled or unfilled.

$$\varepsilon = \left[\frac{235}{f_y}\frac{E}{210\,000}\right]^{0.5} \quad (2)$$

where E is the initial stiffness of stainless steel and f_y is taken as the 0.2% proof stress of the material. The Eurocode 4 compressive design resistance of concrete filled CHS columns $N_{\text{EC4,CHS}}$ is given by Eq. (3) and takes account of the interaction between the steel and concrete elements through the two factors η_s and η_c.

$$N_{\text{EC4,CHS}} = A_s\eta_s f_y + A_c f_c\left[1+\eta_c\left(\frac{t}{D}\right)\left(\frac{f_y}{f_c}\right)\right] \quad (3)$$

where D is the outer diameter of the steel tube, t is the thickness of the steel tube and η_s and η_c are functions of the column slenderness which, for pure compression, are given by Eqs. (4) and (5), respectively. The other symbols are as defined for Eq. (1).

$$\eta_s = 0.25(3+2\bar{\lambda}) \quad (\text{but } \leq 1.0) \quad (4)$$

$$\eta_c = 4.9 - 18.5\bar{\lambda} + 17\bar{\lambda}^2 \quad (\text{but } \geq 0) \quad (5)$$

where $\bar{\lambda}$ is the non-dimensional column slenderness, defined as the square root of the ratio between the plastic cross-sectional resistance and elastic member buckling resistance. The composite columns examined in this study are all of low slenderness ($\bar{\lambda} < 0.1$).

4.3. ACI

The American Concrete Institute (ACI) design guidance [3] for concrete filled tubular sections does not differentiate between section type, and does not make explicit allowance for concrete confinement effects. The compressive design resistance N_{ACI} for all concrete filled tubular sections is given by Eq. (6):

$$N_{\text{ACI}} = 0.85A_c f_c + A_s f_y \quad (6)$$

where the symbols are as previously defined.

4.4. Continuous Strength Method

The Continuous Strength Method (CSM) is a new deformation-based design approach for metallic structures, whereby structural resistance is determined by means of a continuous relationship between cross-section slenderness and deformation capacity in a representative constitutive model. Cross-section slenderness is defined by the maximum plate slenderness $\bar{\lambda}_p = (f_y/\sigma_{cr})^{0.5}$ for SHS and RHS, and by $\bar{\lambda}_c = f_y/\sigma_{cr}$ for CHS, where σ_{cr} is the elastic buckling stress of the element. The corresponding normalised deformation capacity of the section $\varepsilon_{\text{LB}}/\varepsilon_0$ is acquired by means of Eq. (7) for SHS and RHS and Eq. (8) for CHS, where ε_{LB} represents the local buckling strain of the section and ε_0 is the elastic strain at the material 0.2% proof stress, equal to $\sigma_{0.2}/E$.

$$\frac{\varepsilon_{\text{LB}}}{\varepsilon_0} = \frac{1.43}{\bar{\lambda}_p^{2.71-0.686\bar{\lambda}_p}} \quad (7)$$

$$\frac{\varepsilon_{\text{LB}}}{\varepsilon_0} = \frac{0.178}{\bar{\lambda}_c^{1.24+1.70\bar{\lambda}_c}}. \quad (8)$$

The above relationships were derived on the basis of regression analyses through a series of stub column test results. Once the deformation capacity of the section ε_{LB} has been found, the corresponding local buckling stress σ_{LB} may be obtained from a representative material model, for which the compound Ramberg–Osgood model outlined in Section 3.3 is appropriate for stainless steel. The compression resistance of an unfilled stainless steel cross-section is then given by Eq. (9):

$$N_{\text{CSM,Unfilled}} = A_s\sigma_{\text{LB}}. \quad (9)$$

It is proposed that the concept of the Continuous Strength Method may be extended to cover concrete filled tubular sections, and that the compressive resistance may be defined for all tubular sections (N_{CSM}) by Eq. (10), and specifically for CHS ($N_{\text{CSM,CHS}}$) by Eq. (11).

$$N_{\text{CSM}} = A_c f_c + A_s\sigma_{\text{LB}} \quad (10)$$

$$N_{\text{CSM,CHS}} = A_s\eta_s\sigma_{\text{LB}} + A_c f_c\left[1+\eta_c\left(\frac{t}{D}\right)\left(\frac{f_y}{f_c}\right)\right]. \quad (11)$$

In both cases (Eqs. (9) and (10)), the contribution of the stainless steel tube has been modified simply by replacing f_y (taken as the 0.2% proof strength for stainless steel) by the local buckling strength σ_{LB}. It is proposed that the 0.2% proof strength be maintained in the confinement term.

4.5. Comparisons and recommendations

The ultimate loads achieved in the composite stub column tests performed in this study, together with those reported by Young and Ellobody [41], have been summarised in Tables 5 and 6, and compared with the predicted resistance from Eurocode 4, ACI and the CSM. The measured geometry and material properties have been used in all predictions, and the effective area A_{eff} has been used in place of the gross area for the slender (Class 4) stainless steel sections. For the calculation of cross-sectional areas, internal corner radii were assumed to be equal to the material thickness in the absence of measured values. Effective areas were determined in accordance with Eurocode 3: Part 1.5 [48] and the ASCE Specification for stainless steel [51], as appropriate. For some of the stocky CHS, the ultimate loads were associated with high plastic strains; the level of strain that is acceptable will generally depend on the type of structure and the design situation being considered — accidental design situations, for example, will have more relaxed deformation requirements. In this study, the ultimate load carrying capacity attained at or below 5% strain (or 15 mm end shortening of the stub columns), $N_{\text{Test(5\%)}}$, has been taken as the basis for comparison with the design models. This limit on deformation effects the results of three tests — CHS 114 × 6 (Empty), CHS 114 × 6 – C30, and CHS 114 × 6 – C60.

The comparisons of Tables 5 and 6 indicate that the design models previously developed for concrete filled carbon steel tubular sections may generally be safely adopted for concrete filled stainless steel tubes. Indeed, for SHS and CHS, the mean predictions of Eurocode 4 and the ACI design model exhibit close agreement with the test results. On average, the unmodified Continuous Strength Method over-predicts the test capacities, particularly for the high concrete strengths. To reflect this, the following modification (Eq. (12)), whereby the composite resistance is reduced by a factor $\psi = (1 - f_c/900)$ with f_c being in MPa, is proposed. For a concrete strength of 90 MPa, this modification yields a 10% reduction in capacity. The modified CSM resistance $N_{\text{CSM,Mod}}$ provides good agreement with test results and low scatter in the predictions.

$$N_{\text{CSM,Mod}} = \psi(A_c f_c + A_s\sigma_{\text{LB}}). \quad (12)$$

For CHS, existing design guidance is rather conservative, with average test results exceeding design capacities by some margin. Of the existing design models, the Eurocode 4 CHS design model (Eq. (3)) provides the most consistent predictions. Overall, the CSM predictions are the most accurate and consistent, due largely to more accurate assessment of the contribution of the stainless steel tube.

5. Conclusions

Concrete filled tubes are gaining increasing usage in modern construction practice, and with greater emphasis now being placed on durability and life-cycle costing, the use of stainless steel as a structural material is also growing. This paper focuses on the compressive response and design of concrete filled stainless steel tubular sections. A total of 16 stub columns were tested – 8 SHS and 8 CHS – with varying infill concrete strengths. The results, together with the supporting material and geometry properties, have been reported. Comparisons of attained capacities from the tests presented herein, together with other available results from the literature, have been made with existing design models for composite carbon steel sections – Eurocode 4, ACI – and the Continuous Strength Method. Overall, it was found that existing design guidance may generally be safely applied to concrete filled stainless steel tubes, though overly conservative results were apparent, particularly for CHS. The Continuous Strength Method provided the most accurate and consistent prediction of test capacity, due largely to the more precise assessment of the contribution of the stainless steel tube to the composite resistance. This investigation has focused on cross-section capacity, and further experimental and analytical research is required to verify the applicability of the approaches at member level.

Acknowledgements

The authors would like to acknowledge Outokumpu and Stalatube for supplying the stainless steel test specimens. The skilled assistance provided by the technical staff in the School of Civil Engineering at Leeds University is also greatly appreciated.

References

[1] Packer JA, Henderson JE. Hollow structural section connections and trusses — A design guide. Toronto, Canada: Canadian Institute of Steel Construction (CISC); 2003.
[2] Gardner L, Cruise RB, Sok CP, Krishnan K, Ministro dos Santos J. Life cycle costing of metallic structures. Proceedings of the Institution of Civil Engineers — Engineering Sustainability 2007;60(4):166–77.
[3] ACI 318. Building code requirements for structural concrete. Detroit: American Concrete Institute; 1995.
[4] EN 1994-1-1, Eurocode 4: Design of composite steel and concrete structures, Part 1-1 : General rules and rules for buildings. CEN, 2004.
[5] Shanmugam NE, Lakshmi B. State of the art report on steel-concrete composite columns. Journal of Constructional Steel Research 2001;57:1041–80.
[6] Schneider SP. Axially loaded concrete-filled steel tubes. Journal of Structural Engineering, ASCE 1998;10:1125–38.
[7] Lam D, Giakoumelis G. Axial Capacity of circular concrete filled tube columns. Journal of Constructional Steel Research 2004;60:1049–68.
[8] O'Shea MD, Bridge RQ. Design of circular thin-walled concrete filled steel tubes. Journal of Structural Engineering, ASCE 2000;126(11):1295–303.
[9] O'Shea MD, Bridge RQ. the design for local buckling of concrete filled steel tubes. In: Composite construction — conventional and innovate. Austria: Innsbruck; 1997. p. 319–24.
[10] Sakino K, Tomii M, Watanabe K. Sustaining load capacity of plain concrete stub columns by circular steel tubes. In: Conference on concrete filled steel tubular construction; 1998, p. 112–18.
[11] Han LH, Yang Y. Influence of concrete compaction on the behaviour of concrete filled steel tubes with rectangular sections. Advances in Structural Engineering 2001;4(2):93–108.
[12] Han LH, Yao GH. Experimental behaviour of thin walled hollow structural steel (HSS) columns filled with self consolidating concrete (SCC). Journal of Thin Walled Structures 2004;42:1357–77.
[13] Uy B. Concrete filled fabricated steel box columns for multi-storey buildings. Progress in Structural Engineering and Materials 1998;1(2):150–8.
[14] Gibbons C, Scott D. Composite hollow steel tubular columns filled with high strength concrete. In: Proceedings international conference on advances in steel structures; 1996, p. 467–76.
[15] Rangan BV, Joyce M. Strength of eccentrically loaded lender steel tubular columns filled with high strength concrete. ACI Structural Journal 1992;89(b): 676–81.
[16] O'Shea MD, Bridge RQ. Circular thin walled tubes with high strength concrete infill. Composite Construction in Steel and Concrete III ASCE 1996;780–93.
[17] Kilpatrick AE, Rangan BV. Tests on high strength composite concrete columns. Research Report No 1/97, Western Australia: School of Civil Eng., Uni. of Tech.; 1997.
[18] Uy B. Local and post-local buckling of concrete filled steel welded box columns. Journal of Constructional Steel Research 1998;74(1–2):47–72.
[19] Uy B. Static long-term effects in short concrete-filled steel box columns under sustained loading. ACI Structural Journal 2001;98(1):96–104.
[20] Uy B. Strength of short concrete filled high strength steel box columns. Journal of Constructional Steel Research 2001;57(2):113–34.
[21] Han LH, Yao GH. Influence of concrete compaction on the strength of concrete-filled steel RHS columns. Journal of Constructional Steel Research 2003;6: 751–67.
[22] Mursi M, Uy B. Strength of concrete filled steel box columns incorporating interaction buckling. Journal of Structural Engineering, ASCE 2003;129(5): 626–39.
[23] Lam D, Williams CA. Experimental study on concrete filled square hollow sections. Steel and Composite Structures 2004;4(2):95–112.
[24] Han LH. Tests on stub columns of concrete-filled RHS sections. Journal of Constructional Steel Research 2002;58(3):353–72.
[25] Gardner L. The use of stainless steel in structures. Progress in Structural Engineering and Materials 2005;7(2):45–55.
[26] Rasmussen KJR, Hancock GJ. Design of cold-formed stainless steel tubular members I: Columns. Journal of Structural Engineering, ASCE 1993;119(8): 2349–67.
[27] Rasmussen KJR, Hancock GJ. Design of cold-formed stainless steel tubular members. II: Beams. Journal of Structural Engineering, ASCE 1993;119(8): 2368–86.
[28] Talja A, Salmi P. Design of stainless steel RHS beams, columns and beam-columns. Research Note 1619. VTT Building Technology. Finland; 1995.
[29] Young B, Hartono W. Compression tests of stainless steel tubular members. Journal of Structural Engineering, ASCE 2002;128(8):754–61.
[30] Gardner L, Nethercot DA. Experiments on stainless steel hollow sections — Part 1: Material and cross-sectional behaviour. Journal of Constructional Steel Research 2004;60(9):1291–318.
[31] Gardner L, Nethercot DA. Experiments on stainless steel hollow sections — Part 2: Member behaviour of columns and beams. Journal of Constructional Steel Research 2004;60(9):1319–32.
[32] Gardner L, Nethercot DA. Numerical modelling of stainless steel structural components — A consistent approach. Journal of Structural Engineering, ASCE 2004;130(10):1586–601.
[33] Young B, Ellobody E. Column design of cold-formed stainless steel slender circular hollow sections. Steel and Composite Structures 2006;6(4):285–302.
[34] Gardner L, Ashraf M. Structural design for non-linear metallic materials. Engineering Structures 2006;28(6):926–34.
[35] Ashraf M, Gardner L, Nethercot DA. Structural stainless steel design: Resistance based on deformation capacity. Journal of Structural Engineering, ASCE 2008; 134(3):402–11.
[36] Gardner L. The continuous strength method. Proceedings of the Institution of Civil Engineers — Structures and Buildings [submitted for publication].
[37] Young B, Lui WM. Behaviour of cold-formed high strength stainless steel sections. Journal of Structural Engineering, ASCE 2005;131(11):1738–45.
[38] Ellobody E, Young B. Structural performance of cold-formed high strength stainless steel columns. Journal of Constructional Steel Research 2005;61(12): 1631–49.
[39] Gardner L, Talja A, Baddoo NR. Structural design of high strength austenitic stainless steel. Thin-Walled Structures 2006;44(5):517–28.
[40] EN 1993-1-4. Eurocode 3. Design of steel structures: Part 1–4: General rules — Supplementary rules for stainless steels. CEN, 2006.
[41] Young B, Ellobody E. Experimental investigation of concrete-filled cold-formed high strength stainless steel tube columns. Journal of Constructional Steel Research 2006;62:484–92.
[42] Ellobody E, Young B. Design and behaviour of concrete-filled cold-formed stainless steel tube columns. Engineering Structures 2006;28:716–28.
[43] EN 10002-1, Metallic materials —Tensile testing, Part 1: Method of test at ambient temperature. London: British Standards Institution; 2001.
[44] Ramberg W, Osgood WR. Description of stress strain curves by three parameters. Technical note no. 902. Washington, DC: National Advisory Committee for Aeronautics; 1943.
[45] Hill HN. Determination of stress–strain relations from the offset yield strength values. Technical Note No. 927. Washington, DC: National Advisory Committee for Aeronautics; 1944.
[46] Mirambell E, Real E. On the calculation of deflections in structural stainless steel beams: An experimental and numerical investigation. Journal of Constructional Steel Research 2000;54(1):109–33.
[47] Rasmussen KJR. Full-range stress–strain curves for stainless steel alloys. Journal of Constructional Steel Research 2003;59(1):47–61.
[48] EN 1993-1-5. Eurocode 3: Design of steel structures – Part 1–5: General – Strength and stability of planar plated structures without transverse loading. CEN, 2006.
[49] Galambos TV. Guide to stability design criteria for metal structures. 4th ed. New York: John Wiley & Sons, Inc.; 1998. Structural Stability Research Council.
[50] Gardner L, Theofanous M. Discrete and continuous treatment of local buckling in stainless steel elements, Journal of Constructional Steel Research [submitted for publication].
[51] ASCE specification for the design of cold-formed stainless steel structural members, SEI/ASCE 8-02. (Standard No. 02-008). New York: American Society of Civil Engineers; 2002.